Positive and Negative Electrorheological Response of Alginate Salts Dispersed Suspensions under Electric Field

Young Gun Ko,[†] Hyun Jeong Lee,[†,‡] Yong Jin Chun,[§] Ung Su Choi,*[,†] and Ki Pung Yoo[‡]

[†]Center for Urban Energy Systems, Korea Institute of Science and Technology, Hwarangno 14-gil 5, Seongbuk-gu, Seoul 136-791, Korea

[‡]Department of Chemical and Biomolecular Engineering, Sogang University, 35 Baekbeom-ro, Mapo-gu, Seoul 121-742, Korea

[§]Department of Cosmetic Science, Chungwoon University, Daehakgil-25, Hongseong-eup, Hongseong-gun, Chungnam 350-701, Korea

Ⓢ *Supporting Information*

ABSTRACT: Electrorheological (ER) effects of alginic acid and alginate salts (Na^+ alginate, NH_4^+ alginate, and Ca^{2+} alginate) dispersed suspensions were investigated under DC electric fields. A noteworthy result is that the Ca^{2+} alginate dispersed suspension showed negative electrorheological effects under electric fields while the other suspensions exhibited positive electrorheological effects. It is the first time that the negative ER effect is obtained with the biomacromolecule. Interestingly, at the DC electric fields, the electromigration of particles to two electrodes was observed in the negative ER fluid, while the particles-bridges formed between two electrodes in the case of the positive ER fluid. In conclusion, the specific salt type of biomacromolecules could be suitable ER particles for negative ER suspension. We believe that our study can present a new way for the development of the biocompatible and eco-friendly negative ER fluids.

KEYWORDS: *alginates, electric field, electrogelation, electro-response, negative electrorheology*
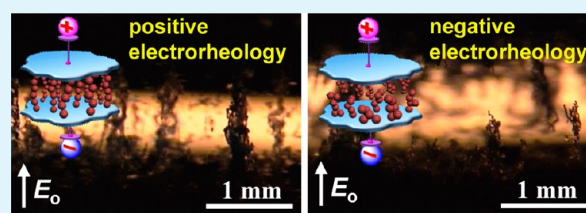
INTRODUCTION

Electrorheological (ER) fluids, composed of small particles dispersed in liquids, have been studied for a half century or more and recently have received much attention due to their potential applications in many industrial areas.[1] Some smart materials can respond to an external environmental stimulus in a timely manner, producing a useful effect.[2] The ER fluids are such smart materials whose rheological properties are controllable through the application of an electric field, showing useful and special function with the effect of reversibility.[3] Most ER devices are designed on the basis of the viscosity change of the ER fluid under the electric field. Clutches,[4] damping devices,[5] and shock absorbers[6] have been studied since the ER effect was reported by Winslow.[7] New promising devices, including ER haptic devices,[8] microfluidic chips,[9] and microfluidic pumps,[10] have been developed. Recently, new combined technology of electrical discharge machining with polishing using ER fluid as working fluid was also developed.[11]

Many efforts have been spent on developing high-performance ER materials to address many problems, for example, a narrow working temperature, sedimentation of ER particles in the liquid medium, solidification at low temperature, a high current density due to the high conductivity of water and device erosion caused by water.[12] The recent issue is the nontoxic and eco-friendly material. The natural polymers have various merits such as biodegradation property, abundant supply, and easy chemical modification for the application to the ER material.[13]

Chitosan, cellulose, and starch have been studied well for their application to ER materials as biodegradable biomacromolecules.[14−18] In biomacromolecules, alginic acid and alginate salts have not been reported yet as the ER material. Alginic acid, also called algin or alginate, is an unbranched polysaccharide consisting of 1→4 linked β-D-mannuronic acid (M) and its C-5 epimer α-L-guluronic acid (G). It is both a biopolymer and a polyelectrolyte that is considered to be biocompatible, nontoxic, nonimmunogenic, and biodegradable. Commercially available alginate is typically extracted from marine brown algae. Due to the abundance of algae in water, there is a large amount of alginate material present in nature.[19−21]

Herein, we present the ER effect of alginic acid and alginate salts dispersed suspensions under DC electric fields. In this study, sodium alginate, ammonium alginate, and calcium alginate were used as the alginate salts to investigate effects of ion, electrical properties, and ionic cross-linking, respectively. When proton ion in the alginic acid is replaced with sodium ion, the wettability and the ion mobility of alginic acid change. Ammonium ion and urea are well-known as a promoter of ER effect due to electrical properties.[22] The molecular chain of alginic acid is cross-linked ionically with calcium ion.[23] The above-mentioned parameters can influence ER properties. This

paper focused on effects of various ion salts for enhancing ER properties of alginic acid dispersed suspension.

Positive ER materials have rheological properties (such as viscosity, shear stress, etc.) that dramatically increase with the applied electric field. In contrast, some ER materials show reverse effect of positive ER materials. They are called negative ER materials.[24] Elongated goethite (β-FeOOH),[25] swollen silicone/BaTiO$_3$ gels,[26] segmented polyurethane,[27] poly(methyl methacrylate) (PMMA),[28] magnesium hydroxide,[29] poly-(tetraflufluoroethylene),[30] and 4-methoxybenzylidene-4′-n-butylaniline[31] were found to show the negative ER effect. However, no natural polymers have been reported as the negative ER material. Various models were suggested to explain negative ER effects. Boissy et al. suggested that the mechanism had an electrophoretic effect.[28] Wu and Conrad provided additional information on the negative ER effect and suggested that electrophoretic- or dielectrophoretic-like effect may not exist or that is very small.[30] Hao et al. introduced the dielectric loss model, according to which the formation of particle chains is possible only if the polarized particles can become reoriented in the field direction.[32] In this paper, we did not suggest a new model for the negative ER effect. However, we believe that our presented data and the pictures of the ER particles in the fluid under DC electric fields can be very useful to develop a new model or present an example of negative ER effect based on the biomacromolecule.

■ EXPERIMENTAL SECTION

Materials. Alginic acid, sodium alginate (Na$^+$ alginate), ammonium alginate (NH$_4^+$ alginate), and calcium alginate (Ca^{2+} alginate) were purchased from Acros Organics, Aldrich, Wako Pure Chemical Industries, and Sigma, respectively, and were used without further purification. All alginic acid and alginate salts particles were freeze-dried for 1 week before use and used promptly before absorbing water. Silicone oil (KF-96-50CS) was purchased from Shin-Etsu Chemical, whose viscosity was 50 mm^2/s at 25 °C. The silicone oil was dried using molecular sieves before use.

Particle Characterization. The alginic acid and alginate salts were ground to 5−50 μm particles using a ball mill. Attenuated total reflectance Fourier transform infrared (ATR FT-IR) was used to analyze samples with a Frontier spectrometer (PerkinElmer) with a diamond coated KRS-5 crystal (PerkinElmer, Universal Diamond ATR). Thermogravimetric analysis (TGA) was performed on the alginic acid and alginate salts using a Q500 thermogravimetric analyzer (TA Instrument) with a heating rate of 10 °C/min under a nitrogen atmosphere from 30 to 900 °C. A field-emission gun scanning electron microscope (FEG-SEM, FEI Inspect F50) was used to observe the morphology of the alginic acid and alginate salts particles. A thin layer of Pt/Pd was sputtered onto the samples prior to imaging using a sputter coater (Hitachi E-1010). The particles elemental analysis was determined by energy dispersive X-ray spectroscopy (EDS) using an EDAX APOLLO XL equipment attached to the FEG-SEM.

Suspension Preparation and Electrorheological Measurements. The ER fluids were prepared by dispersing the alginic acid and alginate salts particles into silicone oil. Two 100 mL of measuring cylinders were prepared. One was filled with 30 mL of ER particle (apparent volume), and the other was filled with 70 mL of silicone oil. Then, the 70 mL of silicone oil was poured into the ER particle filled measuring cylinder. The mixture was well stirred with the magnetic stirrer. The particle concentration was fixed at 30 vol %. The rheological properties of the suspension were investigated in a static DC field using a Physica Couette-type rheometer (Physica MCR301) with a high-voltage generator. The measuring unit was of a concentric cylindrical type, with a 1 mm gap between the bob and the cup. The shear stresses for the suspensions were measured under electric fields of 0−3 kV/mm at two conditions: one is the various shear rates (10^{-5}−1000 s^{-1}) and the fixed temperature (25 °C), and the other is the various temperatures (25−100 °C) and the fixed shear rate (100 s^{-1}). The storage and loss moduli for the suspensions was measured under the frequency of 10^{-2} to 10^2 Hz and electric fields of 0−3 kV/mm at 25 °C.

Electric Characterization of ER Fluids. The DC current density, J, of the alginic acid and alginate salts suspensions were determined at room temperature by measuring the current passing through the fluid upon application of the electric field, E_0, and dividing the current by the area of the electrodes in contact with the fluid. The current was determined from the voltage drop across a 1 MΩ resistor in series with the metal cell containing the oil, using a voltmeter with a sensitivity of 0.01 mV (Keithley, Model 248 High Voltage Supply). The DC conductivity was taken to be ($\sigma = J/E_0$). The dielectric constant, ε, of the suspensions was measured at 0.1−100 kHz and 1000 mV using a Hewlett-Packard LCR meter (model 4263B). Ten samples were measured in order to ensure the reproducibility of the results.
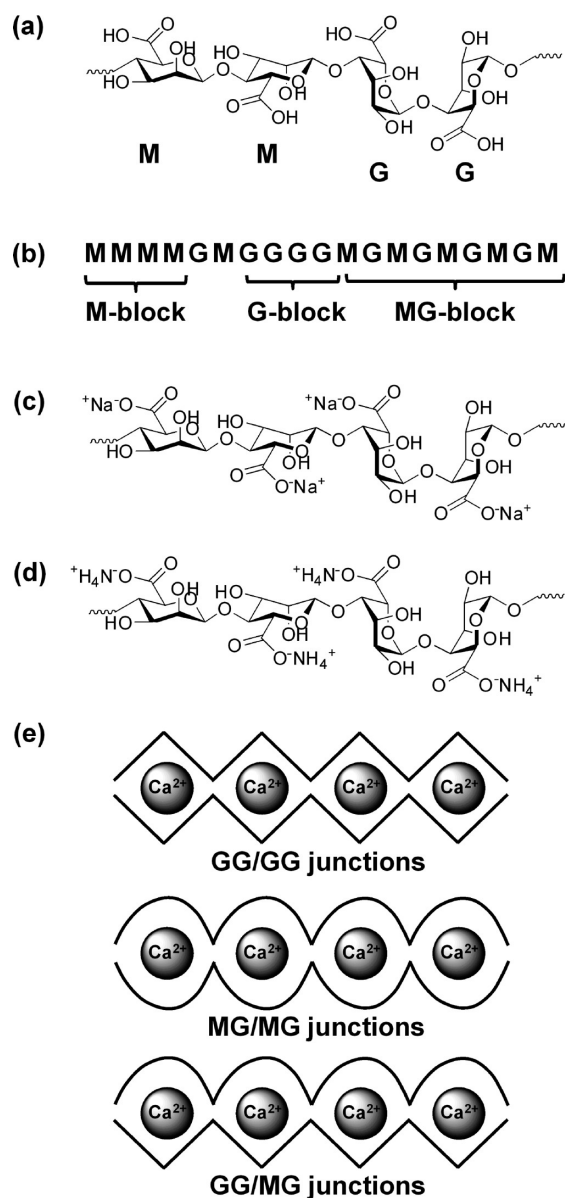
Observation of Structural Patterns of Particles in ER Fluids under DC Electric Field. Mean particle diameter (Heywood diameter, defined as the diameter of a circle having the same area of the segmented defect) of samples was determined by a digital optical microscope (Reichert Metaplan 2, Leica) equipped with a software (Nex Measure Pro 5, Bestecvision, Korea) automatically. The experimental cell was assembled by mounting two parallel electrodes with a 1.5 mm gap on a glass slide, in which a drop of well-mixed ER fluid was dispersed. The behavior of the ER fluids was observed at various DC electric fields using a digital optical microscope.

Particle Dispersion Stability Test. The dispersion stability test of the dispersed suspensions was carried out by UV/vis absorption at the wavelength of 535 nm with UV/visible spectroscopy (Opron-3000, Hanson technology, Korea). Changes in the absorbed UV ray passed through a given spot of the prepared suspensions were measured in accordance with time (0 to ∼1000 h). A decrease in the absorbance with time at a given point implies that sedimentation of the suspension is occurring. The particle concentration was fixed at 5 vol %.

■ RESULTS AND DISCUSSION

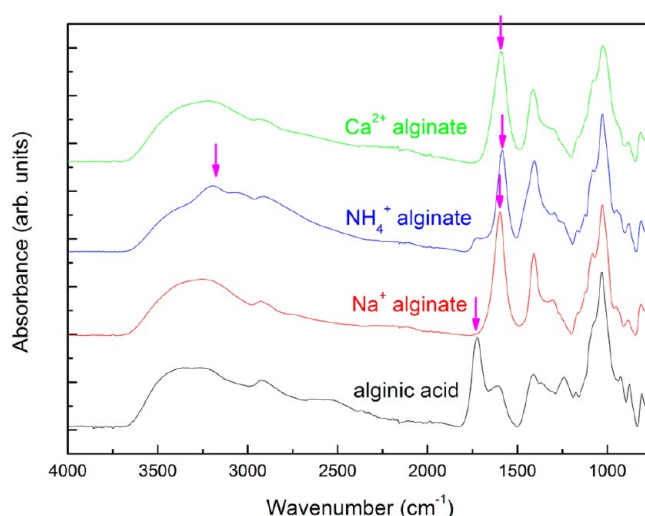**Characterization of Alginic Acid and Alginate Salts.** Alginic acid can be a copolymer composed of mannuronic acid (M block) and guluronic acid (G block) units (Figure 1a) arranged in an irregular blockwise pattern of varying proportions of GG, MG, and MM blocks (Figure 1b).[33] Fractionation yielded a soluble (hydrolyzable) fraction and an insoluble (resistant) fraction. The resistant fractions consisted of molecules which had either mainly M rich or mainly G rich residues, while the hydrolyzable fractions consisted of a high proportion of alternating MG residues. A structure was therefore proposed which consisted of M blocks, G blocks, and hydrolyzable MG alternating blocks. The mannuronic acid forms β (1→4) linkages, so that M block segments show linear and flexible conformation; the guluronic acid, differently, gives rise to α (1→4) linkages, which serves to introduce a steric hindrance around the carboxyl groups. For this reason, the G block segments provide folded and rigid structural conformations that are responsible for a pronounced stiffness of the molecular chains.[19] In this study, alginate salts (Figure 1c−e) were also used as ER materials. Gelation of the alginic acid can be performed by linking to specific and strong interactions between long stretches of G blocks and divalent cations such as Ca^{2+}. Three junctions can be considered as a mechanism of the gelation (Figure 1e). In addition to G blocks, MG blocks also participate, forming weak junctions. Thus, alginates with high G contents yield stronger gels. In the generally accepted model, referred to as an egg-box model, divalent cations promote association of pairs of polymer chains (GG/GG junctions in Figure 1e).[34]

Figure 2. ATR FT-IR spectra for alginic acid, Na$^+$ alginate, NH$_4^+$ alginate, and Ca^{2+} alginate.

Figure 1. Structures of (a) alginic acid, (b) block distribution of alginic acid, (c) Na$^+$ alginate, (d) NH$_4^+$ alginate, and (e) possible junction points in Ca^{2+} alginates.

Chemical structures of the alginic acid and alginate salts were confirmed by ATR FT-IR spectra (Figure 2). Carboxyl group in the alginic acid was confirmed with the peak of asymmetric C=O stretch at 1724 cm^{-1}. This peak disappeared after the reaction with cations, such as Na$^+$, NH$_4^+$, and Ca^{2+}, and new peaks arose at 1597, 1584, and 1589 cm^{-1} due to the carboxyl salt groups (asymmetric CO$_2^-$ stretch) in Na$^+$ alginate, NH$_4^+$ alginate, and Ca^{2+} alginate, respectively. Especially, the peaks for NH$_4^+$···CO$_2^-$ in NH$_4^+$ alginate appeared at around 3000 cm^{-1}. Thermal stability is one of the important factors for ER materials. The thermal analysis using TGA indicates that all alginic acid and alginate salts show the thermal stability under ca. 200 °C. (See Figure 1S in the Supporting Information.)

The alginic acid and alginate salts particles were observed using FEG-SEM (Figure 3a–d). In order to study the elemental composition of the alginic acid and alginate salts, qualitative analysis was performed by energy dispersive X-ray spectroscopy analysis (EDS). The spectrum obtained from EDS analysis showed specific peaks corresponding to the element (Na, N, and Ca) of the cation (Na$^+$, NH$_4^+$, and Ca^{2+}) in each alginate salt (insets in Figure 3b–d). Figure 3e shows the particle-size distribution of the alginic acid and alginate salts. Specific viscous behavior of ER fluids could be observed under an electric field due to the influence of particle size,[35] and the ER effect is weak if the particles are too small, as Brownian motion tends to compete with particle fibrillation. Very large particles are also expected to display a weak ER effect, as sedimentation would prevent the particles from fibrillation bridges.[36] All ER particles have similar size distribution, and the average sizes of the ER particles are ca. 34 μm (diameter).

Electrogelation of Alginic Acid and Alginate Salts Dispersed Suspensions under Electric Fields. The alignment of ER particles in the fluid was observed using an optical microscope with 5 vol % of alginic acid suspension (Figure 4). The experimental cell was assembled by mounting two parallel electrodes with a 1.5 mm gap on a Teflon slide, in which a drop of well-mixed ER fluid was dispersed. The behavior of the ER fluids was observed under 0−2 kV/mm using a digital optical microscope. The presence of fibrils is obvious as the electric field increases, although they are not always linear and even have double loops in some cases. ER particles are aligned under the electric field, and fibrillar shapes of the aligned ER particles flow along the fluids by shear stress. These chains inhibit fluid flow and consequently increase apparent viscosity of the fluid in milliseconds. On the other hand, the viscosity of the fluid recovers the original state promptly by removing the applied field.[37] Generally, two different mechanisms have been proposed to explain the ER phenomena. The electrostatic polarization mechanism, proposed originally by Winslow, attributes the origin of the ER effect to the field-induced polarization of the disperse phase particles relative to the continuous phase. In this model's most general form, polarization can arise from a number of charge transport mechanisms, including electronic, atomic, Debye, or interfacial polarization. Another proposed mechanism is the overlap of electric double layers. Each particle is surrounded by a diffuse counterion cloud that balances its charge (an electric double layer). Under the applied field, this cloud will distort and overlap with the counterion clouds of its neighbors.[38]
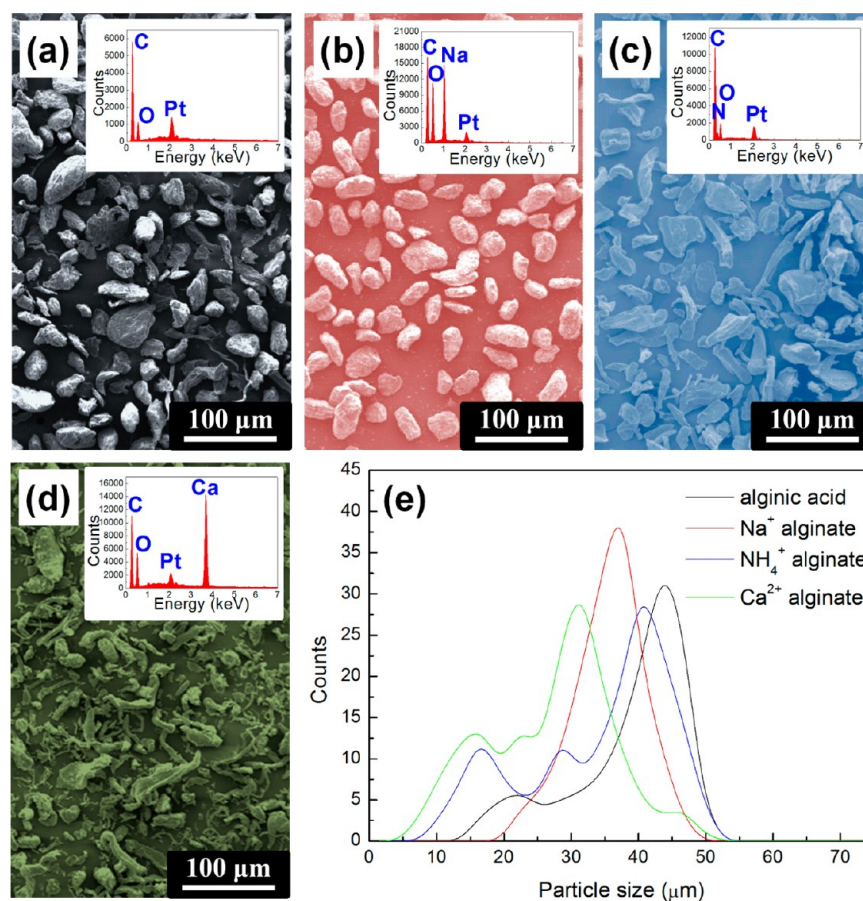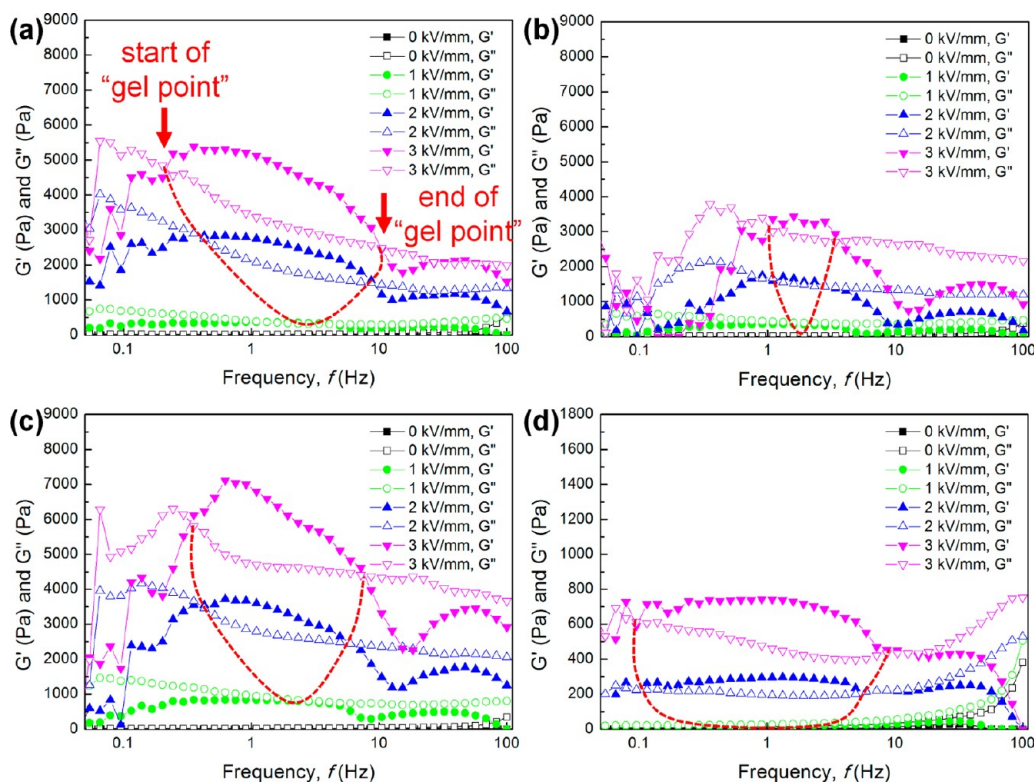
Figure 3. FEG-SEM images and EDS spectra of (a) alginic acid, (b) Na^+ alginate, (c) NH_4^+ alginate, and (d) Ca^{2+} alginate. (e) The particle size distribution of alginic acid and alginate salts.
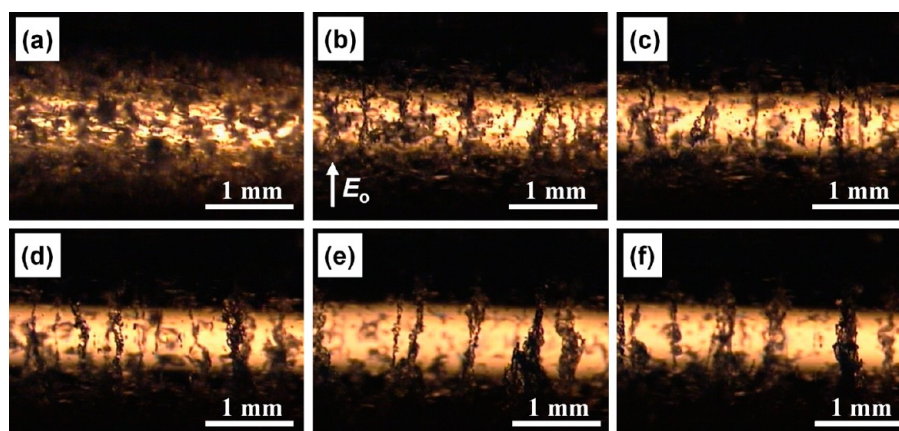
Figure 4. Optical microscopy images of the alginic acid dispersed suspension after application of (a) 0 kV/mm, (b) 0.2 kV/mm, (c) 0.5 kV/mm, (d) 1 kV/mm, (e) 1.5 kV/mm, and (f) 2 kV/mm DC electric fields.

It is well-known that the precise definition of the gel state is somewhat subjective. The criterion depends on changes in the arbitrarily chosen mechanical or structural property measured and on the technique used to make the measurement. A gel may be defined as a material having a loss modulus G'' considerably smaller than the storage modulus G' for several decades of frequency or less restrictively when G' is greater than G'' at some fixed frequency.[39] It is intuitively expected that the cessation of tracer particle motion in a gelling system should correlate with the rheological measurements. The gelation points calculated from the bulk rheology are indicated in Figure 5, defined as the frequency when G' is greater than G''. Red dotted curves represent the region of the gel state at moduli curves. In all prepared fluids, the gel state was observed except for both low and high frequencies after the application of a DC electric field. The region of the frequency for the gel state of all ER fluids under an electric field increased with the increase of the electric field. The Na^+ alginate dispersed suspension showed lower values of G' and G'' and narrower region of the gel state than the alginic acid, while the NH_4^+ alginate dispersed suspension exhibited higher values of G' and

Figure 5. Effect of frequency on storage modulus (G') and loss modulus (G'') for (a) alginic acid, (b) Na^+ alginate, (c) NH_4^+ alginate, and (d) Ca^{2+} alginate dispersed suspensions at room temperature (25 °C). The particle concentration of each ER fluid is 30 vol %. Red dotted curves represent the region of the gel state at moduli curves.

G''. However, in the case of Ca^{2+} alginate fluids, their G' and G'' values are low at all measured frequency regions.

Electrorheological and Electrical Properties of Alginic Acid and Alginate Salts Dispersed Suspensions. Shear stress is one of the critical design parameters in the ER phenomenon and has attracted considerable attention both theoretically and experimentally. Shear stress curves as a function of shear rate for alginic acid and alginate salts dispersed suspensions under 0−3 kV/mm electric field are shown in Figure 2S. (See Supporting Information.) All alginic acid and alginate salts dispersed suspensions showed the typical Bingham plastic behavior except Ca^{2+} alginate. A noteworthy result is that the Ca^{2+} alginate dispersed suspension showed the decrease of shear stress as the increase of the DC electric field, while other prepared ER fluids showed the increase of shear stress as the increase of the DC electric field in the order of NH_4^+ alginate, alginic acid, and Na^+ alginate.

The yield stresses obtained from various logarithmic shear stress versus shear rate curves is also plotted as a function of electric field strength for ER fluids as shown in Figure 6. Electric field-induced shear stress (τ_y) is linearly related to E^2 as mentioned by Marshall et al.: $\tau_y \propto E^2$.[40] This trend is induced by E and also in accordance with theoretical predictions proposed by Klingenberg and Zukoski: $\tau_y \propto E^\alpha$.[41] However, positive ER materials (alginic acid, Na^+ alginate, and NH_4^+ alginate) showed two slopes in the measured electric fields. E_c represents the critical electric field which distinguishes the slopes. E_c was calculated by the linear model fitting and was ca. 1 kV/mm for alginic acid and Na^+ alginate (ca. 1.5 kV/mm for NH_4^+ alginate). In the low electric field region, the α values of alginic acid, Na^+ alginate, and NH_4^+ alginate were +1.330, +1.087, and +1.873, respectively, and in the high electric field
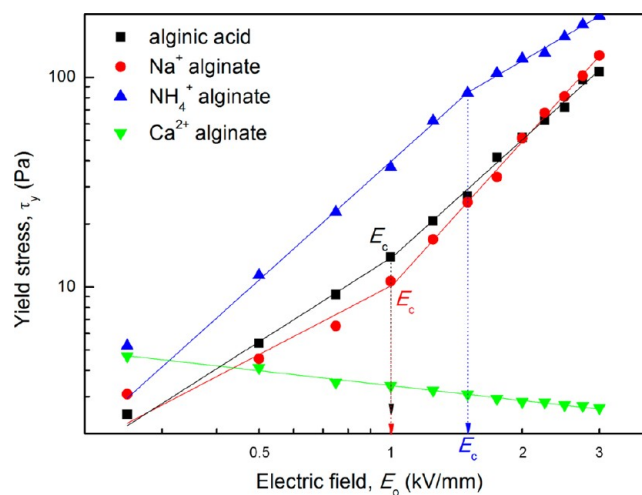
Figure 6. Log−log plot of yield stresses versus electric field for (a) alginic acid, (b) Na^+ alginate, (c) NH_4^+ alginate, and (d) Ca^{2+} alginate dispersed suspensions.

region, their values were +1.887, +2.313, and +1.21, respectively. At the high electric field strength, the electrical response of the fluid becomes nonlinear due to electrical breakdown (or partial discharge). Choi et al. suggest a yield stress scaling function based on nonlinear conductivity model.[42] In the model, the α value is 2 at $E_o \ll E_c$ and is 3/2 at $E_o \gg E_c$. However, our obtained α values differ from the theoretical prediction. The difference is due to several factors, such as particle concentration,[43] shape of the particle,[44] lost of ER effect,[45] etc, and interestingly, α value of Ca^{2+} alginate was −0.236 regardless of the electric field region unlike the other
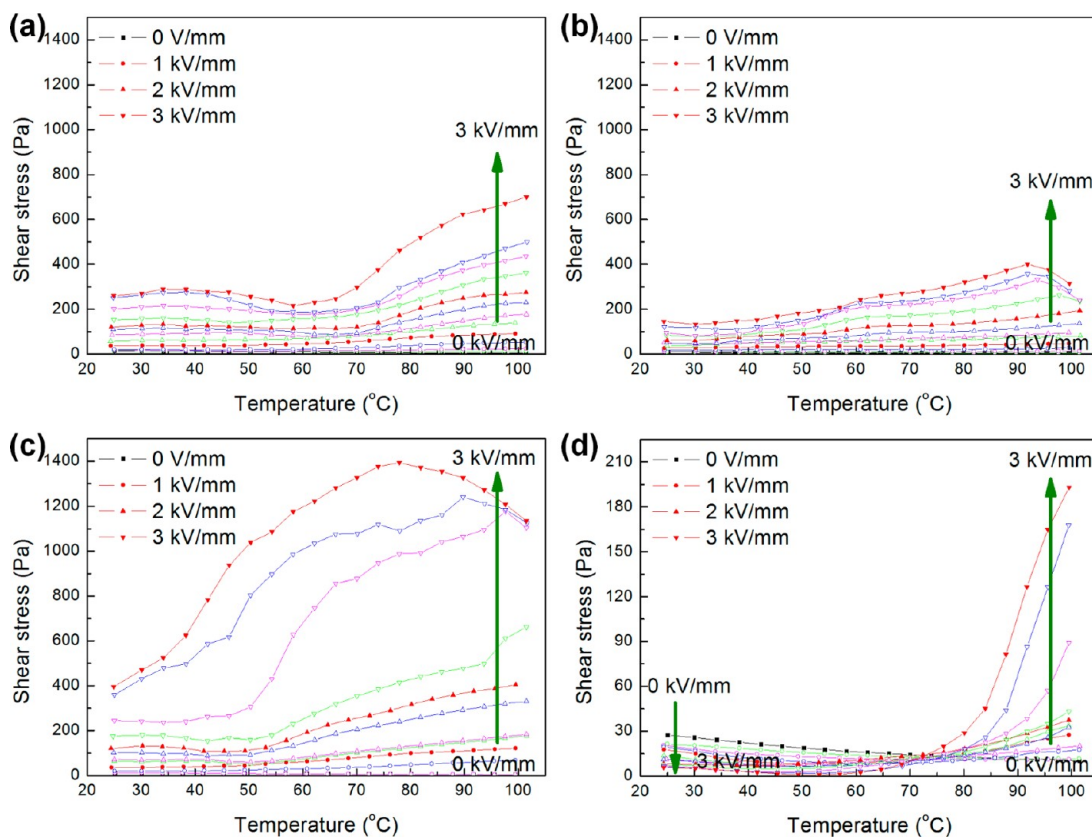
Figure 7. Effect of temperature on shear stress for (a) alginic acid, (b) Na$^+$ alginate, (c) NH$_4^+$ alginate, and (d) Ca^{2+} alginate dispersed suspensions at fixed shear rate (100 s^{-1}) with increments of 0.25 kV/mm. The particle concentration of each ER fluid is 30 vol %.

ER materials. The negative value means that the ER fluid shows the negative electrorheological behaviors.

Dielectric loss model is one of the various models such as fibrillation model, electric double layer (EDL) model, water/surfactant bridge mechanism, polarization model, conduction model, and dielectric loss model to explain the ER phenomena.[24] Two dynamic processes were emphasized in this model. The first step is the particle polarization process, in which the particle dielectric constant is dominant. The second step is particle turning, i.e., the polarized particle could have the capability to align along the direction of the electric field. This step was determined by the particle dielectric loss. The second step is the most important one, which distinguishes the ER particle from non-ER particle. Therefore, dielectric constant is a very important factor for the alginic acid and alginate salts dispersed suspensions as an ER fluid. The dielectric constants of the alginic acid and alginate salts dispersed suspensions were dependent on the frequency of the applied electric field except Ca^{2+} alginate (see Figure S3 in the Supporting Information), and the dielectric constant of NH$_4^+$ doped alginic acid (NH$_4^+$ alginate) was higher than other materials due to the dielectric effect of ammonium ion molecules. The high dielectric constant value of the ER particle implies that the mobile ions tend to accumulate on the surface of the particle.[46] The ionic mobility is related to the mobility of doped molecules and the coordination of carboxyl groups of the chain in the alginic acid. In the prepared ER fluids, the Ca^{2+} alginate dispersed suspension showed higher current density and conductivity than the other fluids. (See Figures S4 and S5 in the Supporting Information.) The current density and the conductivity of all suspensions were lower than 1.0 μA/cm^2 and 30 × 10^{-10} S/m

at the electric field of 3 kV/mm. Therefore, the conductivity is not a significant factor for the application of the alginic acid and alginate salts in the industrial fields.

Figure 7 shows the changes in the shear stress of alginic acid and alginate salts dispersed suspensions under various temperatures and at constant conditions (E_o = 0−3 kV/mm with the gap of 0.25 kV/mm, $\dot{\gamma}$ = 100 s^{-1}, concentration of particles in silicone oil = 30 vol %). The influence of temperature on shear stress may be viewed as deriving from the net effect of two contributions: one is the change in the electrostatic polarization force, which may either strengthen or weaken the ER effect, and the other is the enhancement of Brownian thermal forces at high temperature which tends to weaken the ER effect.[47] Choi et al. suggested that several factors are associated with the temperature effect on the ER performance:[48] (a) increased temperature tends to increase the current density and the increased dielectric constant or conductivity then enhances the particle's polarization, resulting in increased ER performance, (b) increased temperature intensifies the thermal motion of the dispersed ER particles, which leads to lower stability and accordingly degrades the ER performance, and (c) decreased medium viscosity due to temperature increase makes chain formation relatively easy and thus leads to improved ER fluid strength. Whether temperature increase would intensify or weaken the ER effect is really dependent on which factor would become dominant at that temperature. It was observed that the shear stress of the alginic acid dispersed suspension examined in this work increased with the increase of the temperature (Figure 7a). The result in the case of the alginic acid suggests that the polarizability increases with temperature to an extent that dominates over the contribution from Brownian motion

due to the large particle size. However, in the case of Na^+ alginate and NH_4^+ alginate, the polarizability of particles in the range of high temperature decreases due to the high conductivity, and this phenomenon leads to the decrease of the ER effect of the suspension (Figure 7b,c). Adsorbed water on alginate salts also can influence the shear stress during evaporation at high temperature, although all samples were dried in a freeze-dryer for a long time to remove the effect of adsorbed water on ER particles. (All dried samples showed less than 2 wt % of water sorption.) If the adsorbed water is a significant factor for the decrease of the shear stress at the high temperature, the shear stress curve obtained at the low electric field would also show the decreased tendency at the high temperature. However, it was not observed for Na^+ alginate and NH_4^+ alginate dispersed suspensions. Therefore, the decrease of the shear stress at the high electric field might be caused by the high conductivity. The Ca^{2+} alginate dispersed suspension showed interesting electrorheological property (Figure 7d). At the low temperature region, its shear stresses decrease with the electric field and the temperature. However, at the high temperature, they showed the reverse tendency (green arrows in Figure 7d). The Ca^{2+} alginate dispersed suspension exhibited the negative eletrorheological behavior at the low temperature and the positive eletrorheological behavior at the high temperature. At the high temperature, the conductivity of the ER particles increases with the increase of the temperature. Therefore, the increased conductivity of particles overcomes the Quincke rotation of ER particle which causes the negative ER effect and induces the viscosity increase of the fluid. In Figure 7d, the critical temperature for the changing moment from the negative ER to the positive ER is ca. 75 °C.

One of the main challenges in ER investigations is in the selection of the well-dispersed ER suspension. The dispersion stability can be suitably assessed by monitoring: (a) surface charge, (b) sedimentation events, and (c) presence of agglomerates, through time. If the dispersion is unstable, then we expect: (a) lower zeta-potential values (irrespective of polarity), (b) an increase in particle size with time as particles agglomerate, and (c) a decrease in particle concentration with time in the upper dispersion layer as larger agglomerates sediment out.[49] In this study, the sedimentation ratio of particles in the silicone oil was measured according to the elapsed time using UV/vis spectroscopy. In the dispersion stability test, the alginic acid and alginate salts dispersed suspensions showed high dispersion stability for a long time (Figure 8). The dispersion stability of the ER suspensions might be described in the following order: NH_4^+ alginate > alginic acid > Ca^{2+} alginate > Na^+ alginate.

Negative Electrorheological Properties of Calcium Alginate Dispersed Suspension. As the research results shown in front (see Figure 2S, in the Supporting Information, and Figure 6), the Ca^{2+} alginate dispersed suspension showed the negative electrorheological properties. In the polarization model,[50] the attractive force between the particles is proportional to the square of the applied electric field E_o and the dielectric mismatch parameter $\beta_\varepsilon = (\varepsilon_p - \varepsilon_f)/(\varepsilon_p + 2\varepsilon_f)$, where ε_p and ε_f are the real components of the electric permittivities of the particles and the host fluid, respectively. The conduction model[51] considers that the ER effect is induced by the mismatch of the conductivity of the particles and host fluid in DC fields, $\Gamma = \sigma_p/\sigma_f$. When $\sigma_p < \sigma_f$, the apparent viscosity of the whole suspension decreases as the external electric fields increase. Wu and Conrad provide additional information on the
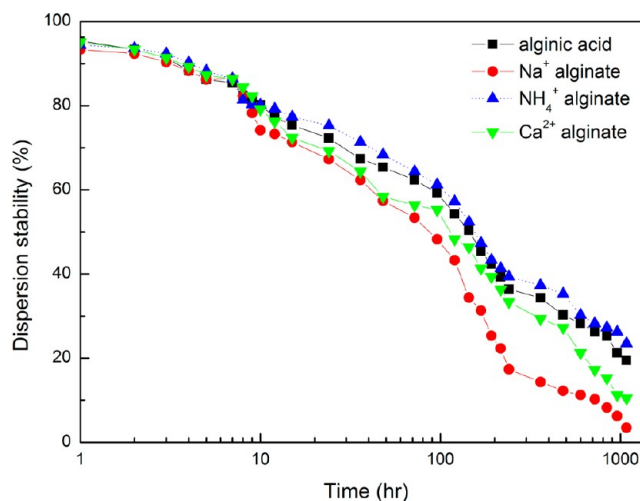

Figure 8. Dispersion stability of the alginic acid and alginate salts particles in silicone oil.

negative ER effect[52] that if both $\sigma_p > \sigma_f$ and $\varepsilon_p > \varepsilon_f$, then the ER response is always positive. In the opposite case ($\sigma_p < \sigma_f$ and $\varepsilon_p < \varepsilon_f$), a negative ER response can be expected. In summary, the ER response will be negative if $\sigma_p < \sigma_f$ and $\varepsilon_p < \varepsilon_f$ or if $\sigma_p \ll \sigma_f$ and $\varepsilon_p > \varepsilon_f$. However, σ and ε of the Ca^{2+} alginate particle is higher than those of the silicone oil. Therefore, the above theories cannot be applied to explain the negative electrorheological behavior of the Ca^{2+} alginate dispersed suspension.

The yield stress, the shear stress, and the apparent viscosity of an ER suspension are largely dependent on the particle volume fraction. In this study, 10, 20, 30, and 40 vol % of Ca^{2+} alginate dispersed suspensions were measured at various electric fields. (See Figure S6 in the Supporting Information.) At the low particle volume fraction (10 and 20 vol %), the negative electrorheological (ER) behavior of the Ca^{2+} alginate dispersed suspensions changed to the positive behavior with the increase of the electric field. However, at the high particle volume fraction (30 and 40 vol %), the suspensions showed only the negative ER behavior. The effect of the particle volume fraction on the ER behavior is clearly observed at the yield stress data (Figure 9). In summary, the negative ER properties of Ca^{2+} alginate dispersed suspension increase with the increase of the particle volume fraction.

The alignment of ER particles in the fluid was observed using an optical microscope with 5 vol % of the Ca^{2+} alginate dispersed suspension (Figure 10). The presence of fibrils is obvious at the two electrodes as the electric field increases, although they are not always linear and even have double loops. However, the fibrils at the two electrodes do not connect each other while the alginic acid dispersed suspension showed connected fibrils between two electrodes as shown in Figure 4. The ER particles electromigrated to either electrode in our experiment. This differs from results published by other researchers, who found migration to just one of the electrodes.[28,52] However, several studies showed the same results as ours.[25,53] The particles in suspension move in response to an electrical field only if they carry a charge. Feng et al. summarized that particle charging and subsequent electrophoretic migration can occur because of one or more of the following phenomena:[53] (a) selective adsorption of ions onto the particles, (b) dissociation of ions from the solid particles, (c) adsorption of dipolar molecules at the surface of

1128

dx.doi.org/10.1021/am302891w | ACS Appl. Mater. Interfaces 2013, 5, 1122–1130
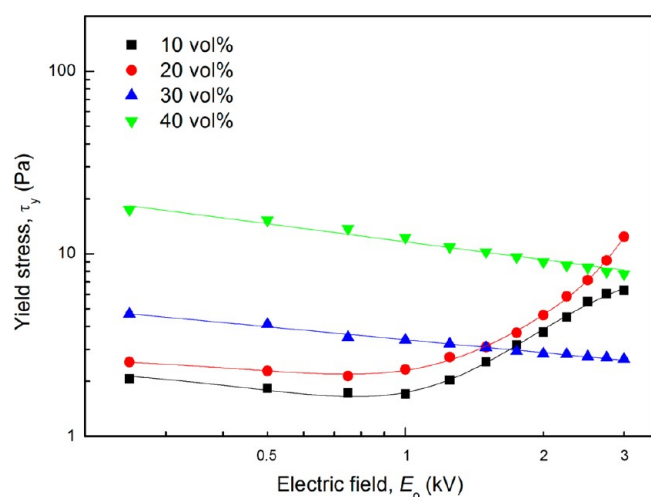
Figure 9. Log–log plot of yield stresses versus electric field for the Ca²⁺ alginate dispersed suspension at various particle volume fractions.

the particles, and (d) electron transfer between the solid and liquid phase due to the differences in work functions, and they also suggested the theory that the aggregation of ER materials on both electrodes originates from an electron transfer among the ER materials under a DC electric field. The shear stress on the shear rate of the Ca²⁺ alginate dispersed suspension decreases with the increase of the electric field due to the electromigration. However, it caused the electrogelation in the suspension and induced the increase of the moduli (G' and G'') of the suspension with the increase of the electric field. Generally, negative ER effects can be achieved by introducing the mechanisms of phase separation of ER fluid and spontaneous electrorotaion or Quincke rotation of ER particle.[54−56] In these possible mechanisms, the mechanism of phase separation was clearly observed as shown in Figure 10.

CONCLUSIONS

In this paper, we presented the ER effect of alginic acid and alginate salts (Na⁺ alginate, NH₄⁺ alginate, and Ca²⁺ alginate) dispersed suspensions under DC electric fields. The Ca²⁺ alginate dispersed suspension showed negative ER effect, while other prepared ER fluids (alginic acid, Na⁺ alginate, and NH₄⁺ alginate dispersed suspensions) showed the positive

ER effect. To our knowledge, it is the first time that the negative ER effect is obtained with biomacromolecules. In the case of positive ER fluid, the alignment of ER particles in the fluid was observed with forming fibrils, and the fibrils were located between two parallel electrodes with connection of the two electrodes. However, in the case of negative ER fluid, the fibrils at the two electrodes do not connect to each other, although the presence of fibrils is obvious at the two electrodes as the electric field increases. The electromigration occurred in the negative ER fluid. These phenomena led the both shear stress and moduli increase with the increase of the electric field in the case of the positive ER fluid while the shear stress decreases in the case of the negative ER fluid. In the negative ER mechanisms of phase separation of ER fluid and spontaneous electrorotation or Quincke rotation of ER particle, the phase separation of ER fluid was clearly observed in this study.

In brief, the results in this study indicate that ER effects of the alginic acid and alginate salts dispersed suspensions depend on the salt type. It is expected that this work on the response of the alginates to the electric stimulus will lay the foundation for the future application to the bioelectric signal between biomacromolecules and cells in addition to electrorheological materials.

ASSOCIATED CONTENT

Ⓢ Supporting Information
TGA curves, shear stress curves on shear rate, and electrical properties of alginic acid and alginate salts dispersed suspensions. This material is available free of charge via the Internet at http://pubs.acs.org.

AUTHOR INFORMATION

Corresponding Author
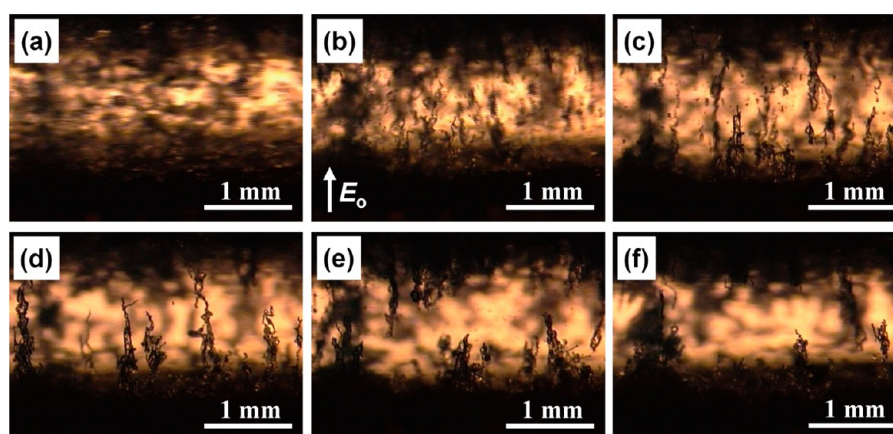*Tel.: 82-2-958-5657. Fax: 82-2-958-5659. E-mail: uschoi@kist.re.kr.

Notes
The authors declare no competing financial interest.

ACKNOWLEDGMENTS

Figure 10. Optical microscopy images of the Ca²⁺ alginate dispersed suspension after application of (a) 0 kV/mm, (b) 0.2 kV/mm, (c) 0.5 kV/mm, (d) 1 kV/mm, (e) 1.5 kV/mm, and (f) 2 kV/mm DC electric fields.

■ REFERENCES

(1) Block, H.; Kelly, J. P. *J. Phys. D: Appl. Phys.* **1988**, *21*, 1661−1677.

(2) Lavalle, P.; Voegel, J.-C.; Vautier, D.; Senger, B.; Schaaf, P.; Ball, V. *Adv. Mater.* **2011**, *23*, 1191−1221.

(3) Whittle, M.; Bullough, W. A. *Nature* **1992**, *358*, 373.

(4) Litvinov, W. G. *IMA J. Appl. Math.* **2008**, *73*, 619−640.

(5) Nguyen, Q.-H.; Choi, S.-B. *Smart Mater. Struct.* **2009**, *18*, 115020.

(6) Wereley, N. M.; Lindler, J.; Rosenfeld, N.; Choi, Y.-T. *Smart Mater. Struct.* **2004**, *13*, 743−752.

(7) Winslow, W. M. *J. Appl. Phys.* **1949**, *20*, 1137−1140.

(8) Han, Y.-M.; Choi, S.-B. *Smart Mater. Struct.* **2008**, *17*, 065012.

(9) Zhang, M.; Wu, J.; Niu, X.; Wen, W.; Sheng, P. *Phys. Rev. E* **2008**, *78*, 066305.

(10) Liu, L.; Chen, X.; Niu, W.; Wen; Sheng, P. *Appl. Phys. Lett.* **2006**, *89*, 083505.

(11) Tsai, Y. Y.; Tseng, C. H.; Chang, C. K. *J. Mater. Process. Technol.* **2008**, *201*, 565−569.

(12) Inoue, A.; Ide, Y.; Oda, H. *J. Appl. Polym. Sci.* **1997**, *64*, 1319−1328.

(13) Ko, Y. G.; Choi, U. S. *Soft Matter* **2012**, *8*, 253−259.

(14) Ko, Y. G.; Shin, S. S.; Choi, U. S.; Park, Y. S.; Woo, J. W. *ACS Appl. Mater. Interfaces* **2011**, *3*, 1289−1298.

(15) Ko, Y. G.; Lee, H. J.; Shin, S. S.; Choi, U. S. *Soft Matter* **2012**, *8*, 6273−6279.

(16) Gindl, W.; Emsenhuber, G.; Maier, G.; Keckes, J. *Biomacromolecules* **2009**, *10*, 1315−1318.

(17) Negita, K.; Itou, H.; Yakou, T. *J. Colloid Interface Sci.* **1999**, *209*, 251−254.

(18) Sung, J. H.; Park, D. P.; Park, B. J.; Choi, H. J.; Jhon, M. S. *Biomacromolecules* **2005**, *6*, 2182−2188.

(19) Yang, J.-S.; Xie, Y.-J.; He, W. *Carbohydr. Polym.* **2011**, *84*, 33−39.

(20) Pawar, S. N.; Edgar, K. J. *Biomaterials* **2012**, *33*, 3279−3305.

(21) Lee, K. Y.; Mooney, D. J. *Prog. Polym. Sci.* **2012**, *37*, 106−126.

(22) Wen, W.; Huang, X.; Yang, S.; Lu, K.; Sheng, P. *Nat. Mater.* **2003**, *2*, 727−730.

(23) Donati, I.; Holtan, S.; Mørch, Y. A.; Borgogna, M.; Dentini, M.; Skjåk-Bræk, G. *Biomacromolecules* **2005**, *6*, 1031−1040.

(24) Hao, T. *Adv. Colloid Interface Sci.* **2002**, *97*, 1−35.

(25) Ramos-Tejada, M. M.; Arroyo, F. J.; Delgado, A. V. *Langmuir* **2010**, *26*, 16833−16840.

(26) Mitsumata, T.; Sugitani, K. *Macromol. Rapid Commun.* **2004**, *25*, 848−852.

(27) Kimura, H.; Aikawa, K.; Masubuchi, Y.; Takimoto, J.; Koyama, K.; Uemura, T. *J. Non-Newtonian Fluid Mech.* **1998**, *76*, 199−211.

(28) Boissy, C.; Atten, P.; Foulc, J.-N. *J. Electrost.* **1995**, *35*, 13−20.

(29) Trlica, J.; Quadrat, O.; Bradna, P.; Pavlinek, V.; Saha, P. *J. Rheol.* **1996**, *40*, 943−946.

(30) Wu, C.; Conrad, H. *J. Rheol.* **1997**, *41*, 267−281.

(31) Negita, K. *Chem. Phys. Lett.* **1995**, *246*, 353−357.

(32) Hao, T.; Kawai, A.; Ikazaki, F. *Langmuir* **2000**, *16*, 3058−3066.

(33) Draget, K. I.; Taylor, C. *Food Hydrocolloids* **2011**, *25*, 251−256.

(34) Sikorski, P.; Mo, F.; Skjåk-Bræk, G.; Stokke, B. T. *Biomacromolecules* **2007**, *8*, 2098−2103.

(35) Ko, Y. G.; Choi, U. S.; Chun, Y. J. *J. Colloid Interface Sci.* **2009**, *335*, 183−188.

(36) Hao, T. *Adv. Mater.* **2001**, *13*, 1847−1857.

(37) Halsey, T. C. *Science* **1992**, *258*, 761−766.

(38) Parthasarathy, M.; Klingenberg, D. J. *Mater. Sci. Eng. R-Rep.* **1996**, *R17*, 57−103.

(39) Moschakis, T.; Murray, B. S.; Dickinson, E. *J. Colloid Interface Sci.* **2010**, *345*, 278−285.

(40) Marshall, L.; Zukoski, C. F.; Goodwin, J. W. *J. Chem. Soc.-Farady Trans. 1* **1989**, *85*, 2785−2795.

(41) Klingenberg, D. J.; Zukoski, C. F. *Langmuir* **1990**, *6*, 15−24.

(42) Choi, H. J.; Cho, M. S.; Kim, J. W.; Kim, C. A.; Jhon, M. S. *Appl. Phys. Lett.* **2001**, *78*, 3806−3808.

(43) Sung, J. H.; Jang, W. H.; Choi, H. J.; Jhon, M. S. *Polymer* **2005**, *46*, 12359−12365.

(44) Kligenberg, D. J.; van Swol, F.; Zukoski, C. F. *J. Chem. Phys.* **1991**, *94*, 6170−6178.

(45) Ko, Y. G.; Chun, Y. J.; Kim, J.-Y.; Choi, U. S. *Colloids Surf., A: Physicochem. Eng. Aspects* **2010**, *371*, 76−80.

(46) Osman, Z.; Ibrahim, Z. A.; Arof, A. K. *Carbohydr. Polym.* **2001**, *44*, 167−173.

(47) Hiamtup, P.; Sirivat, A.; Jamieson, A. M. *J. Colloid Interface Sci.* **2008**, *325*, 122−129.

(48) Kim, S. G.; Lim, J. Y.; Sung, J. H.; Choi, H. J.; Seo, Y. *Polymer* **2007**, *48*, 6622−6631.

(49) Tantra, R.; Jing, S.; Pichaimuthu, S. K.; Walker, N.; Noble, J.; Hackley, V. A. *J. Nanopart. Res.* **2011**, *13*, 3765−3780.

(50) Kligenberg, D. J.; Zukoski, C. F. *Langmuir* **1990**, *6*, 15−24.

(51) Tang, X.; Wu, C.; Conrad, H. *J. Appl. Phys.* **1995**, *78*, 4183−4188.

(52) Wu, C.; Conrad, H. *J. Rheol.* **1997**, *41*, 267−281.

(53) Feng, P.; Wan, Q.; Fu, X. Q.; Wang, T. H. *Appl. Phys. Lett.* **2005**, *87*, 033114.

(54) Huang, H.-F.; Zahn, M.; Lemaire, E. *J. Electrost.* **2011**, *69*, 442−455.

(55) Lobry, L.; Lemaire, E. *J. Electrost.* **1999**, *47*, 61−69.

(56) Lemaire, E.; Lobry, L.; Pannacci, N.; Peters, F. *J. Rheol.* **2008**, *52*, 769−783.